PHYSICAL REVIEW B VOLUME 44, NUMBER 17 1 NOVEMBER 1991-I

Ising model on Penrose lattices: Boundary conditions

Erik Schwartz Sørensen*
Laboratoire Physique Statistique, Ecole Normale Supérieure, 24, rue Lhomond, 75231 Paris CEDEX 05, France

Marko V. Jarić
Center for Theoretical Physics, Texas A&M University, College Station, Texas 77843

Marco Ronchetti
Dipartimento di Fisica, Universitá degli Studi di Trento, 38050 Povo, Italy
(Received 26 March 1991)

The zero-field ferromagnetic Ising model is studied on three different geometries that all approach Penrose lattices. Two types of *aperiodic* boundary conditions are presented. By means of Monte Carlo simulation and finite-size scaling we determine with high accuracy the transition temperature, critical exponents η and ν, specific-heat critical amplitude, and several finite-size-scaling amplitudes, and we study the effects of different boundary conditions. In all cases, we find that $\eta \approx \frac{1}{4}$ and $\nu \approx 1$. Thus, we conclude that, despite its quasiperiodicity, the Ising model on the Penrose lattices belongs to the same universality class as Ising models on periodic lattices. We find that the aperiodic boundary conditions lead to finite-size-scaling functions different from those for periodic boundary conditions. However, the rates of convergence to the finite-size-scaling regime are comparable between different boundary conditions.

I. INTRODUCTION

The present paper is the first of two papers where the zero-field ferromagnetic Ising model on Penrose lattices is studied. We shall present here high-precision Monte Carlo simulations determining the universality class of the model. The Penrose lattices are a family of pentagonal quasiperiodic tilings of the plane. In reality one can only simulate finite systems and, consequently, one must also specify the boundary conditions. For periodic lattices one can always take a finite portion consisting of several unit cells so that the usual, periodic boundary conditions can be applied. Since the Penrose tilings are not periodic, the same approach can be used only by *approximating* a Penrose lattice by periodic tilings with an increasingly larger unit cell. However, in the thermodynamic limit, any such periodic tiling belongs to the usual Ising universality class. If the universality class were to change in the limit of the Penrose tilings, one or more of the (nonuniversal) critical amplitudes of the periodic tilings would have to tend to zero or diverge, leading to different critical exponents. We therefore study the behavior of the exponents *as well as* the critical amplitudes as the Penrose lattices are approached through a sequence of periodic tilings. Second we investigate the effects of three different kinds of boundary conditions on the finite-size scaling. The geometries considered are the rational approximants to the Penrose lattices subject to periodic boundary conditions, topologically a torus, and two types of *aperiodic* boundary conditions, one with a spherical topology and one with a toroidal topology. We shall refer to these geometries as periodic, spherical, and toroidal boundary conditions, respectively. In a planned second paper we shall be concerned with the influence of phason fluctuations on the ferromagnetic transition.

Our investigation is motivated by the discovery of quasicrystals, some of which could undergo a magnetic transition. It is thus of natural interest to study the Ising model on Penrose tilings which are one of the possible conceptual models of quasicrystals. As opposed to the well-known periodic lattices, for some of which the Ising model is solvable in two dimensions, Penrose lattices are quasiperiodic, making any analytical approach very difficult. This quasiperiodicity could lead to a new critical behavior. Mainly this question will be addressed in this paper. On the other hand, there is now experimental evidence that some icosahedral and decagonal Al-Mn-Si alloys are three-dimensional spin glasses.[1] These materials possess a large degree of the so-called phason disorder. This is the main motivation for investigating the effects of phason fluctuations in the Ising model on Penrose lattices, which will be presented in the second of our two papers.

For the one-dimensional quasicrystal, the Fibonacci chain of long and short bonds (tiles), the Ising model in a field is solvable by exact renormalization-group methods.[2,3] If the interactions along the short and long bonds have different signs an interesting rich structure of the ground state is seen. The phonon spectrum of the Fibonacci chain was calculated[4] and observed to have a Cantor set structure. Also the quantum spin-$\frac{1}{2}$ XY Fibonacci chain in zero field is solvable[5] and displays similar properties. For Penrose lattices fewer properties are known. There is substantial evidence that the Ising model on the Penrose lattices should belong to the universality class of the periodic lattices,[6–10] as well as

some evidence that the aperiodicity could lead to a different critical behavior.[11] An Ising model including several couplings has also been considered[12] and recently the antiferromagnetic Ising model on Penrose lattices has been studied.[13] A version of the eight-vertex model on the Penrose lattices was solved by Korepin,[14] and was seen to have properties close to the periodic case. For three-dimensional quasicrystals there are now results showing that $T_c = 4.972 \pm 0.06$.[15]

We shall consider spins $\sigma_i = \pm 1$ located at the vertices of a Penrose lattice [see Fig. 1(a)] and described by the zero-field, ferromagnetic ($J \geq 0$) Ising Hamiltonian

$$H = -J \sum_{<i,j>} \sigma_i \sigma_j , \tag{1}$$

where the sum is over all pairs of spins connected by the edges of the individual rhombi (tiles). Previously, Bhattacharjee, Ho, and Johnson,[16] have performed Monte Carlo simulations of the Ising model on Penrose lattices.

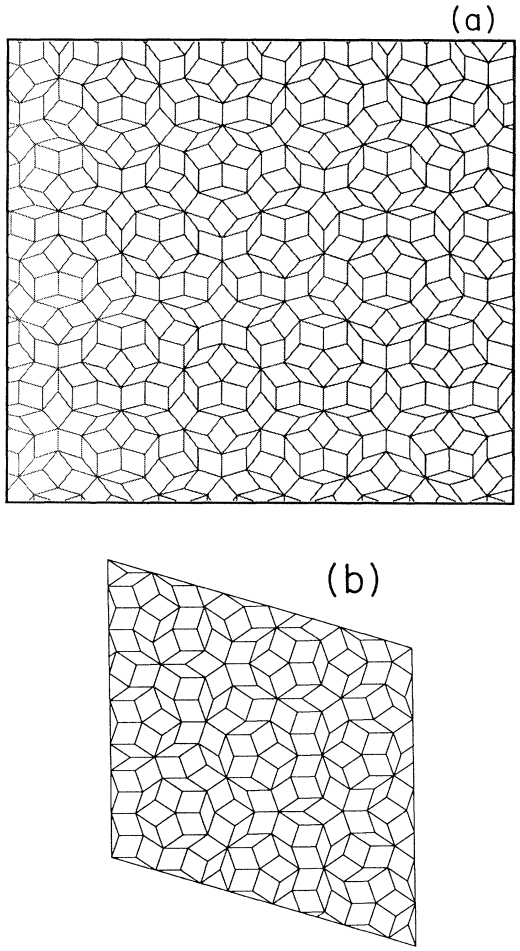

FIG. 1. (a) A section of the Penrose lattice. In our model, spins are located at the vertices and interact along the bonds. (b) Unit cell of the $q = 5$ periodic approximant to the Penrose lattices.

They obtained finite-size data by considering subblocks of a master Penrose lattice. However, since the Penrose lattices do not allow for periodic boundary conditions, they used free boundary conditions which result in a difficulty in the finite-size analysis due to a large "surface" energy caused by the unsatisfied bonds at the free boundary. They obtained the estimate $T_c/J = 2.41 \pm 0.02$ for the transition temperature and observed no change in the universality class away from the square lattice Ising model.

Okabe and Niizeki studied the Ising model both on Penrose lattices[17] and its dual lattices[18] also by Monte Carlo methods. However, rather than considering Penrose lattices themselves, they studied periodic approximations to Penrose lattices, the so-called rational approximants, which allowed them to use the ordinary periodic boundary conditions. These approximants are *periodic* tilings of the plane with a unit cell, such as the one shown in Fig. 1(b), consisting of several Penrose rhombi. A rational approximant is characterized by an integer q. In the limit where q tends to infinity, the unit cell of the approximant becomes infinitely large and one obtains a Penrose lattice. One can now obtain finite systems, such as the ones indicated by shading in Fig. 2, for which the usual periodic boundary conditions can be applied. By considering a sequence indicated in the first column in Fig. 2, i.e., a sequence of *different* rational approximants with increasingly larger unit cells, Okabe and Niizeki[17] applied the usual finite-size scaling analysis and obtained an estimate of the critical temperature,

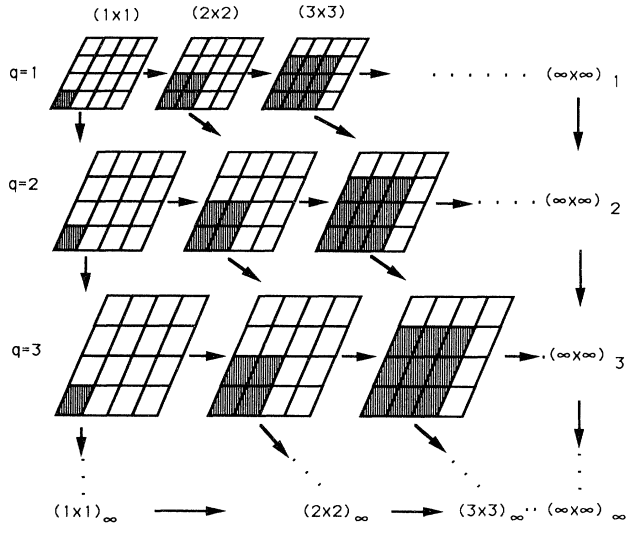

FIG. 2. Schematic presentations of different periodic approximant routes to Penrose tilings. Each row represents a periodic lattice approximating Penrose lattices. It is labeled by an index $q = 1, 2, \ldots$. The rhombic unit cell of each periodic lattice, such as the one shown in Fig. 1(b) for $q = 5$, consists of many Penrose rhombi. The nth column represents finite, $(n \times n)$ unit cells, subsets (shaded) of infinite periodic approximants. Periodic boundary conditions are imposed on the finite Ising models defined on these subsets.

TABLE I. The critical temperature T_c, the exponents η and ν, the specific heat amplitude A_0, the susceptibility amplitude χ_0, and g^* for different boundary conditions.

b.c.	T_c	$1/\nu$	η	A_0	χ_0	g^*
$(2\times 2)_\infty$	2.400±0.002	0.96±0.02	0.242±0.003	0.415±0.012	0.400±0.004	0.912
$(\infty\times\infty)_\infty$	2.401±0.005	1.00±0.01	0.252±0.00?	≈0.43	0.412±0.002	0.916
Spherical	2.398±0.004	1.02±0.01	0.248±0.002	0.444±0.006	0.334±0.002	0.842
Toroidal	2.398±0.002	1.00±0.01	0.246±0.002	0.440±0.006	0.351±0.003	0.845

$2.388 \leq T_c/J \leq 2.396$, and also observed no change in the exponents away from those of the square lattice Ising model. In this way they *simultaneously* approach the Penrose lattices and the thermodynamic limit. However, the finite-size scaling analysis is well understood only for periodic lattices, i.e., for sequences such as the ones corresponding to the rows in Fig. 2. Therefore, it is not *a priori* clear how "good" their finite-size scaling analysis should be. Also in this way it is not possible to study the critical amplitudes as a function of the rational approximants.

In this paper we apply periodic boundary conditions in a different way and we also consider two new types of boundary conditions. As a result we can examine the effect of different boundary conditions on the finite-size scaling analysis, and we obtain accurate predictions for the transition temperature T_c, critical exponents η and ν, and the specific heat critical amplitude A_0. Our results are summarized in Table I, from which we conclude that the ferromagnetic Ising model on Penrose lattices belongs to the same universality class as the Ising model on periodic lattices. The error bars given in the table indicate that the accuracy of all approaches is comparable so that the computationally least expensive one may be used.

The periodic boundary conditions are applied on rational approximants. However, we first extrapolate to the thermodynamic limit for a given rational approximant. That is, we first apply finite-size scaling analysis for *each* rational approximant (each q) by considering a sequence of finite systems of $n \times n$ unit cells, $n \to \infty$ (each row in Fig. 2). Then we extrapolate the results for the sequence of rational approximants to the limiting case of a Penrose lattice ($q \to \infty$). This is illustrated by the last column in Fig. 2. We shall refer to this procedure as the $(\infty \times \infty)_\infty$-periodic boundary conditions. A sequence along the nth column will be referred to as having $(n \times n)_\infty$-periodic boundary conditions, whereas a sequence along the qth row will be referred to as $(\infty \times \infty)_q$-periodic boundary conditions. Thus, Okabe and Niizeki used $(1 \times 1)_\infty$-periodic boundary conditions. We have also analyzed $(2 \times 2)_\infty$-periodic boundary conditions and the results are included in Table I.

Although for a given approximant to the Penrose lattices the unit cell has a rather complicated structure and consists of many individual rhombi, the approximants are still *periodic* lattices. Thus, the approximants should be in the same universality class as the Ising model on the usual periodic lattices. This is indeed the case, as can be seen from the critical exponents listed in Table II. They are not seen to vary appreciably as a function of the approximants. One finds $\eta \approx \frac{1}{4}$ and $\nu \approx 1$. However, as previously mentioned, this does *not* exclude the possibility that Penrose lattices can belong to a different universality class. Namely, as one approaches Penrose lattices, one or more of the critical amplitudes could tend to zero or diverge and thus lead to new critical behavior. It would only be possible to detect this by studying the critical amplitudes or the finite size-scaling amplitudes as a function of the approximants. This is done here by extensive computer simulations. The relevant amplitudes are also listed in Table II, and we see that they approach finite, nonzero numbers in the limit $q \to \infty$. For example, the specific heat critical amplitude is observed to

TABLE II. The critical temperature T_c, the exponents η and ν, the specific heat amplitude A_0, the susceptibility amplitude χ_0, and g^* for different rational approximants characterized by q. The entry for $q = \infty$ corresponds to the extrapolation we refer to as $(\infty \times \infty)_\infty$-boundary conditions in the text.

q	T_c	$1/\nu$	η	A_0	χ_0	g^*
1	2.26918...	1.0	$\frac{1}{4}$	0.494358...	—	~ 0.916
2	2.376±0.004	0.98±0.02	0.237±0.003	0.465±0.011	0.413±0.004	0.922
3	2.390±0.004	1.02±0.02	0.264±0.003	0.465±0.011	0.407±0.004	0.913
4	2.397±0.003	0.98±0.03	0.258±0.003	0.436±0.020	0.414±0.005	0.914
5	2.399±0.002	0.99±0.02	0.250±0.003	0.431±0.011	0.410±0.004	0.914
6	2.398±0.003	1.02±0.02	0.252±0.003	0.432±0.015	0.415±0.005	0.918
∞	2.401±0.005	1.00±0.01	0.252±0.001	≈0.43	0.412±0.002	0.916

decrease, but it saturates at a finite value, $A_0 \approx 0.43$. We also find that T_c, which is not a universal quantity, varies with the approximants. However, its limiting value $T_c/J = 2.401 \pm 0.005$, like the values of ν, η, and A_0, should be independent of the boundary conditions.

The toroidal and spherical boundary conditions are described in detail in the next section. In both cases we consider progressively larger segments of a Penrose lattice and we prescribe the mutual bonding (identification) of the surface spins so as to reduce the large surface energy (which would result from the free boundary conditions) while preserving the local matching rules of Penrose lattices (which are violated in rational approximants). The toroidal boundary conditions correspond to a toroidal geometry with variable radii and one expects similar results as for rational approximants. Indeed, we find $T_c/J = 2.398 \pm 0.002$, $\eta \approx \frac{1}{4}$, $\nu \approx 1$, and $A_0 \approx 0.44$, which are close to the values obtained from rational approximants. The spherical boundary conditions correspond to a spherical geometry and we determine $T_c/J = 2.398 \pm 0.004$, $\eta \approx \frac{1}{4}$, $\nu \approx 1$, and $A_0 \approx 0.44$, which are again close to the values obtained from rational approximants. Therefore, we must conclude that the Ising model on the Penrose lattices belongs to the same universality class as the Ising model on periodic lattices.

In Sec. II we present the model and the different ways of constructing the boundary conditions. Section III describes the numerical simulation procedure and the finite-size scaling analysis. In Sec. IV we discuss the results of the simulation and the finite-size analysis for the approximants and for the toroidal and spherical boundary conditions.

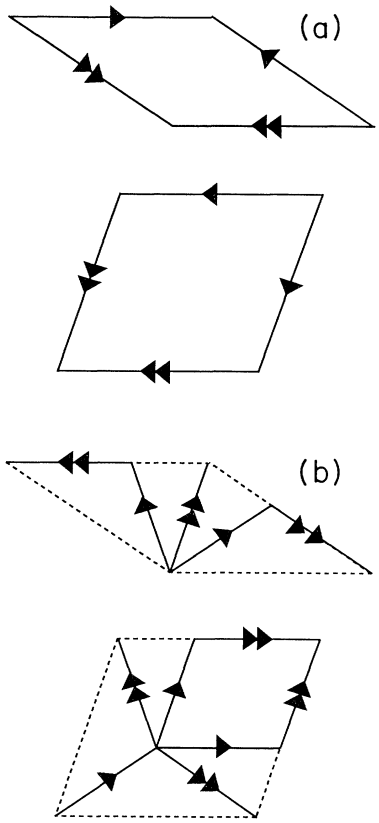

FIG. 3. (a) Arrowed rhombi which force a quasiperiodic tiling of the plane. (b) Inflation of the arrowed rhombi.

II. THE MODEL

We shall not go into much detail about properties and various ways of constructing the Penrose lattices on which our model, Eq. (1), is defined, since that has been done elsewhere, we refer the reader to Ref. 19. Here we shall only recapture some of the basic properties necessary to define finite-size approximations (and their boundary conditions) whose thermodynamic limit is a Penrose lattice. The Penrose lattice shown in Fig. 1(a) can be viewed as a tiling of the plane by 36° and 72° rhombi of unit edge length. Clearly, these two rhombi can tile the plane in many ways, including periodic tilings, such as the one shown in Fig. 1(b). However, if the two rhombi are equipped with arrows, as shown in Fig. 3(a), and the arrows are required to match, the resulting tiling is always a Penrose lattice as shown in Fig. 1(a). This jigsaw puzzle method of constructing a Penrose lattice is not very efficient. The most efficient way is by means of the inflation-deflation transformation, which prescribes a subdivision of the rhombi into rhombi rescaled by the golden mean $\tau = (1 + \sqrt{5})/2$ as shown in Fig. 3(b). As this transformation is iterated *ad infinitum* one obtains a Penrose lattice. Different seeds, i.e., different initial arrangements of tiles, will, under the inflation transformation, generally lead to different Penrose lattices. Of course, for the purpose of computer simulations, we need to find a way of constructing similar sequences of finite systems which reproduce a Penrose lattice in the thermodynamic limit. In order to make the convergence to a Penrose lattice as fast as possible, we first require that the average coordination of spins in our finite systems be as close as possible to 4, the value for the Penrose lattice. For example, if we consider finite systems constructed by the inflation, we see that the average coordination z is reduced from the Penrose lattice value by a term inversely proportional to the length of the boundary (surface), i.e., $z = 4 - O(N^{-1/2})$, where N is the number of spins in the system. This necessary consequence of the free boundary conditions can be improved upon by connecting or identifying pairs of spins from the boundary. However, we should also require that the resulting Hamiltonian consists of quadrangular plaquettes, supplied by arrows as in Fig. 2(a), with as few arrow mismatches and as few new vertex types as possible.

We shall be concerned here only with the boundary conditions which result in a spherical or toroidal topology of the resulting Hamiltonian and we shall consider only few simple cases. The average coordination can be immediately calculated using the Euler characteristics for a given topology and the fact that the Hamiltonian consists of plaquettes which are quadrangles. Thus, $z = 4$ for the torus while $z = 4 - 8N^{-1}$ for the sphere. Therefore, from the point of view of the coordination, one would

expect faster convergence for toroidal topology than for the spherical topology.

A. Rational approximants

The usual method for constructing toroidal boundary conditions is by means of planar periodic approximations of Penrose lattices, the so-called rational approximants. We shall refer to these boundary conditions as periodic, since this is the most natural way of extending the notion of periodic boundary conditions to Penrose lattices. We shall only highlight the discussion of these rational approximants which can be found in Ref. 20. For the rational approximant the tiles are exactly the same as for the regular Penrose lattice, however they are now arranged in a periodic fashion. It should be immediately clear that any planar periodic approximation of a Penrose lattice must contain arrow mismatches. In fact, it is shown in Ref. 20 that each rational approximant has precisely two arrow mismatches and, thus, at least four new vertex types. The unit cell of the rational approximants is spanned by the two basis vectors

$$R^{(1)} = (P\tau + Q)\left(\frac{2\tau - 1}{2}, -\tau^{-1}\sin\frac{\pi}{5}\right), \tag{2}$$

$$R^{(2)} = (P\tau + Q)\left(0, 2\sin\frac{\pi}{5}\right), \tag{3}$$

where

$$\tau = (\sqrt{5} + 1)/2. \tag{4}$$

By choosing P and Q as consecutive numbers from the Fibonnacci sequence

$$P = F_q, \quad Q = F_{q-1}, \tag{5}$$

we obtain the qth approximant. The number of tiles in a unit cell is

$$N_q = F_{2q+1} + 2F_{2q}. \tag{6}$$

In the following we consider approximants with q=1 to 6, which have 4, 11, 29, 76, 199, and 521 rhombi per unit cell, respectively. A unit cell of the $q = 5$ rational approximant is shown in Fig. 1(b). The number of tiles increases by approximately $\tau^2 \approx 2.6$ between subsequent approximants. The number of 36° and 72° rhombi are given by the equations

$$N_{36°} = F_{2q-1} + 2F_{2q-2}, \quad N_{72°} = F_{2q} + 2F_{2q-1}. \tag{7}$$

The ratio $N_{72°}/N_{36°}$ thus approaches the value τ for the Penrose lattices when q tends to infinity.

For a regular Penrose lattice individual sites will have coordination numbers ranging from three through seven, though the average coordination number is *exactly* four. It is interesting to compare T_c for the Penrose lattice and other two-dimensional four-coordinated lattices such as the square lattice ($T_c = 2.26918\ldots$) and the Kagomé lattice ($T_c = 2.1433\ldots$). The first of the approximants, $q = 1$, has only 4-coordinated sites and is thus completely equivalent to the square lattice, although the unit cell consists of three 72° and one 36° rhombi. The second approximant, $q = 2$, has sites of coordination ranging from three through six, with 7-coordinated sites being absent in this approximant. For higher approximants the full range of coordination numbers from three through seven is present. In general, there are two arrow mismatches for the approximants and, therefore, also at least three disallowed vertices. The coordination z is, however, exactly four.

B. Spherical boundary conditions

The simplest way to obtain a spherical boundary condition is by simply identifying spins on matching edges of the 72° (or 36°) rhombus. This procedure naturally carries over to the inflations of the rhombus. However, at certain stages of the inflation, this simplest case leads to other than quadrangular plaquettes. This can be avoided by joining along the matching edges not one but n 72° rhombi. We consider in our simulation the case with $n = 5$, as shown in Fig. 4(a). Here five vertices denoted

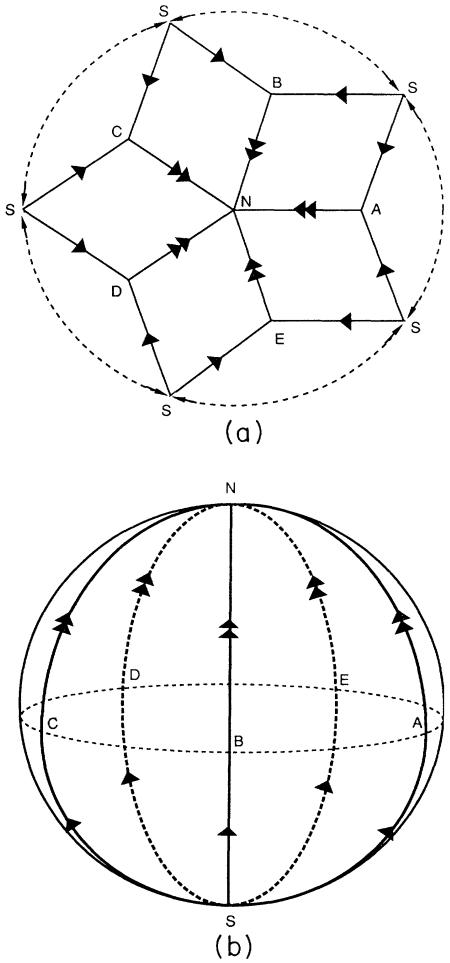

FIG. 4. (a) Identification of spins and edges for "spherical" boundary conditions. The points A, B, C, D, and E correspond to the vertices not found in the Penrose lattices. (b) Graphical illustration of how the five rhombi are joined together to form the "sphere."

by A, B, C, D, and E, of a kind not found in the Penrose lattices, appear along the equatorial plane as shown in Figs. 4(a) and 4(b). For these vertices the sum of the angles is 216° if one considers the tiles as flat and undistorted. On the two poles, denoted by N and S in Fig. 4, the sum of the angles is 360° and the vertex is one of the eight found in the Penrose lattices. Therefore, the resulting structure can be viewed as flat, having five 144° disclinations located at A through E, where the entire curvature of the sphere is concentrated. If we were to use any inflation of n 72° rhombi, $1 < n \neq 5$, joined along the matching edges, we would again get a structure with the matching rules satisfied everywhere, but n disallowed vertices would appear in the equatorial plane, and the vertices on the two poles would also not be among the eight allowed in the Penrose lattices. The third through seventh inflation, of the original five rhombi, that we consider have the following numbers of spins: 107, 277, 722, 1887, and 4937. Here the number of *spins* is given by the relation

$$N_{\text{sphere}} = 5(F_{2q+1} + F_{2q}) + 2, \tag{8}$$

where $q = 0$ corresponds to the original five rhombi, and the Fibonacci numbers, F_q, satisfy the familiar recursion relation

$$F_q = F_{q-1} + F_{q-2}, \quad F_0 = 0, \; F_1 = 1. \tag{9}$$

We shall refer to this as spherical boundary conditions. As mentioned above, these boundary conditions satisfy the arrow matching rules. However, $z \neq 4$, and 5 disallowed vertices occur.

C. Toroidal boundary conditions

We shall discuss here a different method of constructing toroidal boundary conditions. We start with one 72° rhombus which is inflated. The spins on the edges are now identified as shown in Fig. 5(a). We can do this only if the tiles match across the edges. As can be seen in Fig. 5(a), this indeed occurs for the fourth and all subsequent inflations of the 72° rhombus and we will use these inflations in our calculations.[21] In Fig. 5(b) we illustrate how the inflated rhombus is first folded into a "double cone" and subsequently into a torus. Again, all the arrow-matching rules are satisfied, but there are two new vertices, marked A and B in Fig. 5(a) which are not allowed in the Penrose lattices. If one considers flat, undistorted tiles, the sum of the angles at B is 216°, while at A it is 404°. Thus, these two points can be viewed as a pair of ±144° disclinations in a flat, periodic tiling. We used this sequence of finite systems with toroidal boundary conditions with total number of spins equal to 54, 141, 369, 966, and 2529 corresponding to the fourth through eighth inflation. The number of spins, which in this case corresponds to the number of rhombi since the coordination is exactly four, is given by the relation

$$N_{\text{torus}} = F_{2q+1} + F_{2q} - F_{2q-7} - F_{2q-8}. \tag{10}$$

Here q is the inflation number, q=0 for the original rhombus, and q=4 for the first case where one can construct the toroidal boundary conditions. These boundary conditions also satisfy the arrow matching rules, and $z = 4$, however, there are 2 disallowed vertices. We shall refer to these boundary conditions as toroidal.

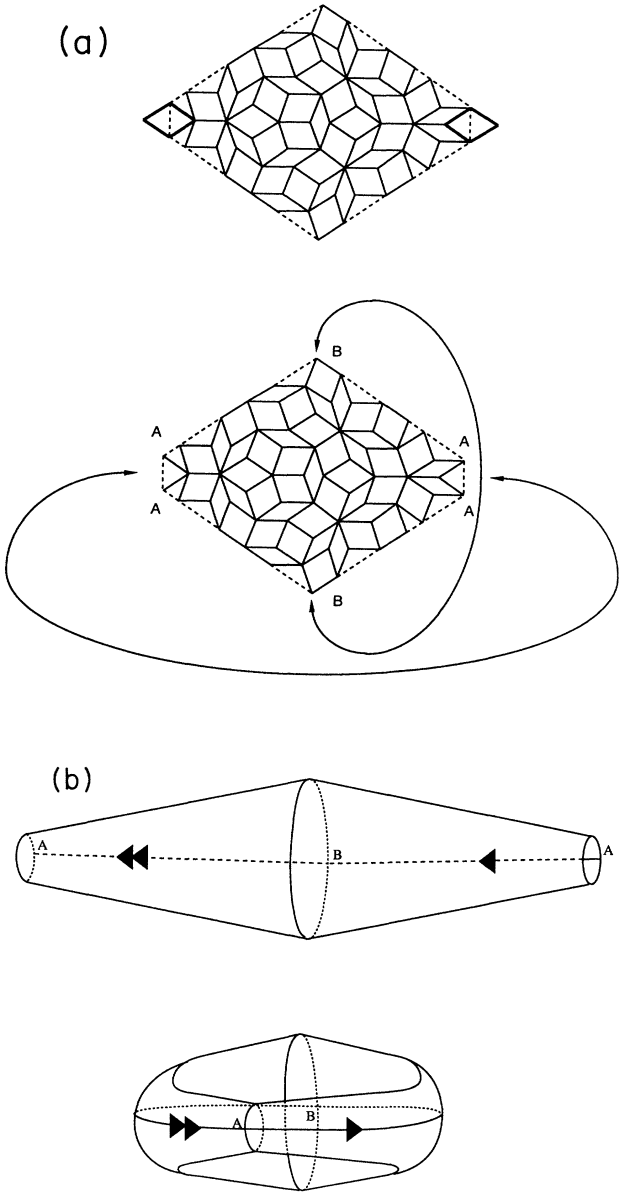

FIG. 5. (a) Fourth inflation of the 72° rhombus and identification of spins appropriate for toroidal boundary conditions used here. (b) Two-step graphical illustration of how a 72° rhombus is folded first into a "double cone" and, then, into a "torus" with nonconstant radii.

III. MONTE CARLO SIMULATION

In order to determine the transition temperature it is necessary to obtain thermodynamic quantities at different temperatures. We use the method of Ferrenberg and Swendsen[22] to do this. A standard Metropolis importance sampling of the system is performed at a temperature close to the transition temperature. For each of the lattices considered the first 10^5 Monte Carlo steps per spin (MC/S) is discarded for equilibration. For the ensuing 2.5×10^6 to 5×10^6 MC/S a measurement of the relevant quantities such as energy and magnetization is written to a file for each 100 MC/S. Thus, the complete Boltzmann distribution of the basic quantities of interest is kept. From this information it is now possible to obtain estimates at nearby temperatures, utilizing the well-known form of the Boltzmann distribution. For example, within the usual framework of importance sampling, where one replaces ensemble averages by "time" averages, one has for a quantity Q:

$$Q(T_0) = \frac{1}{Z(T_0)} \sum_i Q_i, \tag{11}$$

where T_0 is the simulation temperature, $Z(T_0)$ the number of measurements, and Q_i the quantity Q at the ith measurement. If in addition to Q_i, the corresponding energy E_i is stored, one can obtain $Q(T)$ from the following expression:

$$\begin{aligned} Q(T) &= \frac{1}{Z(T)} \sum_i Q_i e^{(1/T_0 - 1/T)E_i}, \\ Z(T) &= \sum_i e^{(1/T_0 - 1/T)E_i}, \end{aligned} \tag{12}$$

where the sum is over the individual measurements. Using this method it is possible to obtain good estimates of thermodynamic quantities for a range of temperatures around the simulation temperature. Unfortunately, this range narrows with increasing lattices sizes. It is, however, only necessary to make the actual simulation at one temperature. Thus, if one has some knowledge of where the transition is one can obtain good results from a single high-quality simulation. For the simulations that we report we have performed substantially longer runs than have been previously reported.[16,17] Another advantage of this method is the possibility of obtaining, at a later time, any quantity defined in terms of the basic variables that were stored. For example, by storing just the distribution of the energy and magnetization the susceptibility and specific heat can be calculated later on. A drawback is, of course, that extra storage space is required.

For the determination of error bars we split the sequence of measurements into bins of 1000 consecutive measurements. Calculations are then performed for each bin giving 25 to 50 nearly independent estimates. The error is then obtained by standard methods.

Although, in contrast to the critical exponents and ratios of certain critical amplitudes, the transition temperature T_c is not universal, it is needed in our method of calculating the critical exponents. Therefore, we need to calculate T_c to a high accuracy. We shall also want to evaluate certain nonuniversal amplitudes, some depending on the boundary conditions.

A convenient way of locating the transition temperature and computing the critical exponents using finite-size data has been discussed by Binder.[23] Here we shall make a similar approach. We study the following ratio of cumulants:

$$g(T, L) = \frac{1}{2}\left(3 - \frac{\langle M^4 \rangle_L}{\langle M^2 \rangle_L^2}\right), \tag{13}$$

where L is the linear system size, M the magnetization, and $\langle \cdot \rangle$ denotes the ensemble average. This ratio of the cumulants has simple properties that make it ideal for determining the transition temperature in a finite-size scaling analysis:

$$\lim_{L \to \infty} g(T, L) = \begin{cases} 0, & T > T_c; \\ 1, & T < T_c. \end{cases} \tag{14}$$

The transition temperature T_c can be obtained by noting that according to finite-size scaling

$$g(T, L) = \tilde{g}\left(tL^{1/\nu}\right), \tag{15}$$

where $t = (T - T_c)/T_c$ is the reduced temperature and, for a given universality class, the function $\tilde{g}$ depends only on the boundary conditions. This implies that $g(T = T_c, L) = \tilde{g}(0) \equiv g^*$ is independent of the system size. Curves for different lattice sizes will, therefore, intersect at the transition temperature. However, unlike T_c, the value of g^* will generally depend on the boundary conditions used.

We can also obtain the correlation length exponent ν from Eq. (15). It follows that

$$g'(T_c, L) = \frac{\tilde{g}'(0)}{T_c} L^{1/\nu}, \tag{16}$$

where g' denotes partial derivative with respect to the temperature. As mentioned above, for the systems in the same universality class the quantity $\tilde{g}'(0)$ should depend only on the boundary conditions. By plotting $\ln|g'(T_c)|$ versus $\ln L$ we should obtain a straight line whose slope is $1/\nu$ and whose intercept with the y axis is $\ln[|\tilde{g}'(0)|/T_c]$.

The exponent η can also be obtained from a finite-size scaling analysis. Here, we make the standard finite-size scaling ansatz[24]

$$\langle M^2 \rangle_L \ |_{T=T_c} \simeq M_0^2 L^{d+2-\eta}, \tag{17}$$

where M is the total magnetization and M_0 is a finite-size scaling amplitude which, for a given universality class, will generally depend on the boundary conditions. Therefore, a log-log plot of $\langle M^2 \rangle$ versus L should be a straight line with the slope $4-\eta$ and the y-axis intersection $\ln M_0^2$.

We also study the specific heat critical amplitude. From the work of Ferdinand and Fisher[25] it is known that the specific heat of the 2D Ising model on a square lattice has the finite-size scaling form

$$C_L(T_c)/k_B = A_0 \ln L + B(0,1) + O\left((\ln L)^3/L^2\right), \tag{18}$$

where A_0 is the same constant as the one describing the divergence of the specific heat for the infinite lattice,

$$C(T)/k_B = A_0 \ln \mid (T/T_c) - 1 \mid + A_1 + O\left([(T/T_C) - 1] \ln \mid (T/T_c) - 1 \mid\right). \tag{19}$$

Thus in this case the finite-size scaling amplitude and the critical amplitude are the same. Ferdinand and Fisher[25] showed that

$$A_0 = (2/\pi)\left[\ln\left(1+\sqrt{2}\right)\right]^2 = 0.494\,358\ldots, \tag{20}$$

$$B(0,1) = 0.138\,149\ldots. \tag{21}$$

Using Eq. (18) as our finite-size scaling ansatz we can determine A_0 by making a semilog plot of the specific heat at T_c as a function of the linear size of the system. A linear dependence will be interpreted in the usual way to mean that the specific heat critical exponent α is zero. Moreover, since the amplitude A_0 is a critical amplitude, it should be independent of the boundary conditions used to calculate it. In the simulations we obtain the specific heat through the relation

$$C_L(T) = T^{-2} L^{-d}\left(\langle E^2\rangle - \langle E\rangle^2\right), \tag{22}$$

where E is the total energy.

In a similar manner one can analyze the susceptibility. We define the susceptibility as

$$\chi_L(T) = \begin{cases} (T)^{-1} L^{-d}\left(\langle M^2\rangle - \langle \mid M \mid\rangle^2\right), & T < T_c; \\ (T)^{-1} L^{-d}\langle M^2\rangle, & T \geq T_c. \end{cases} \tag{23}$$

For a discussion of this definition see Ref. 26. In this case the finite-size scaling ansatz takes the form[27]

$$\chi_L \mid_{T=T_c} \simeq \chi_0 L^{2-\eta}, \tag{24}$$

which follows directly from Eq. (17). Using the value for T_c previously obtained, χ_0 can be extracted from the log-log plot of the susceptibility at T_c as a function of the linear size of the system. For a given universality class, the finite-size scaling amplitude, $\chi_0 = M_0^2/T_c$ is proportional to the susceptibility critical amplitudes $\chi_\pm$ (defined by $\chi \sim \chi_\pm \mid t \mid^{-\gamma}$), but the proportionality constant will generally depend on the boundary conditions, and will be nonuniversal. Thus, χ_0 will depend on the boundary conditions. Depending on which of the two defintions in Eq. (23) one takes at $T = T_c$, determines whether χ_0 is proportional to χ_+ or χ_-.

IV. RESULTS

We start by discussing our results for the periodic boundary conditions constructed using rational approximants. Then, the two other boundary conditions, i.e., spherical and toroidal, will be analyzed. For the simulations subsequently described the temperature is measured in units of the coupling constant J.

A. Periodic boundary conditions

The lattice sizes considered range from $4\times4, 5\times5, 6\times6$, and 7×7 unit cells, for the $q = 2$ approximant, to $1\times1, 2\times2$, and 3×3 unit cells, for the $q = 6$ approximant. In Fig. 6, $g(T)$ is shown for the $q = 5$ approximant. For this approximant we consider lattices of $1\times1, 2\times2, 3\times3$, and 4×4 unit cells. The number of spins in the different lattices is then N=199, 796, 1791, and 3184. The simulation temperature is in this case $T = 2.39$. From the data obtained in this simulation $g(T)$ is then calculated in temperature steps of 0.002. From the intersection of the different curves we can read off the transition temperature, $T_c/J = 2.399 \pm 0.002$, at $g^* \simeq 0.914$.

Using the same method we obtain the transition temperature, as well as g^*, for all the approximants from $q = 2$ to $q = 6$. The obtained values are tabulated in Table II. It is seen that g^* is in the range $0.912 - 0.922$ which is in nice agreement with Monte Carlo as well as renormalization-group results,[24] establishing that for the Ising model on a periodic lattice g^* indeed should be in the range $\approx 0.915 - 0.918$. For the $q = 1$ approximant T_c is the well-known Ising value of $T_c/J = 2.269\ldots$. It is now possible to extrapolate to the limit of a regular Penrose lattice. We make the phenomenological assumption that T_c is some polynomial in $1/q$. Presumably any other quantity that parametrizes the approximants, such as the number of rhombi in the unit cell, would work equally well. A good fit is obtained with the polynomial $2.401 - 0.076q^{-2} - 0.056q^{-3}$ which is shown as a solid line in Fig. 7. In this fit the linear term in q was fixed to zero. The limiting value of $T_c(q)$ is $T_c(\infty) = 2.401 \pm 0.005$. Only a small variation in T_c is observed for the larger approximant, justifying the use of $(1\times1)_\infty$-periodic boundary conditions used by Okabe and Niizeki[17] although our value of T_c is slightly higher.

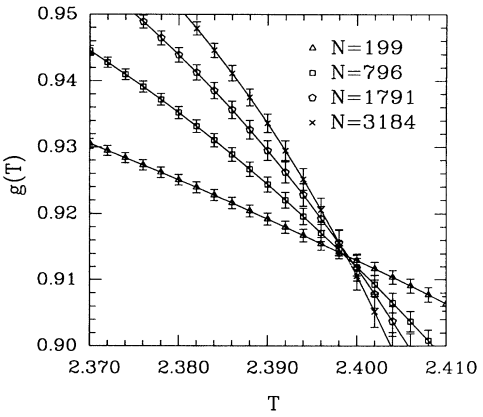

FIG. 6. $g(T)$, defined in the text, as a function of T for the $q = 5$ approximant. The lines shown are for linear sizes of 1, 2, 3, and 4 unit cells, consisting of 199, 796, 1791, and 3184 spins. In all cases 3×10^6 MC/S were performed. The simulation temperature was 2.39.

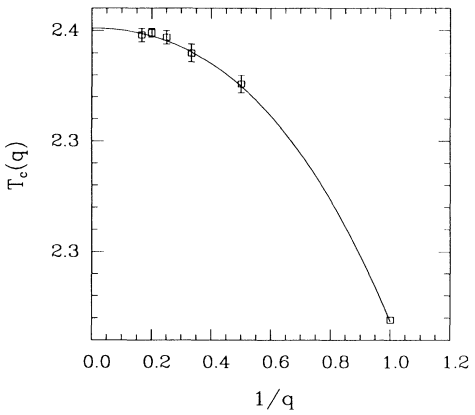

FIG. 7. T_c as a function of q^{-1}. The solid line shown is $2.401 - 0.076q^{-2} - 0.057q^{-3}$. For q=1 this fit passes through the exact T_c of the two-dimensional Ising model on a square lattice.

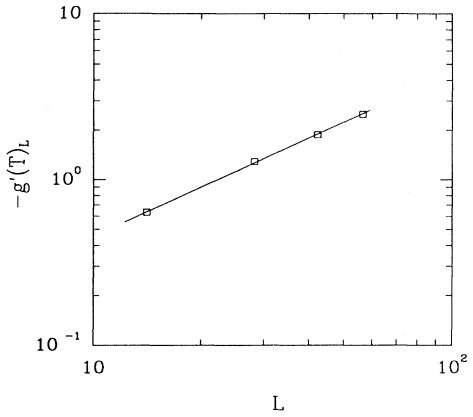

FIG. 9. $g'(T_c)$ as a function of $L = \sqrt{N}$ for the $q = 5$ approximant. The points shown are for linear sizes of 1, 2, 3, and 4 unit cells, with N equal to 199, 796, 1791, and 3184, respectively. In all cases 3×10^6 MC/S were performed. The error bars are smaller than the points shown. The simulation temperature was 2.39.

We have also analyzed our data using the $(2 \times 2)_\infty$-periodic boundary conditions (see Table I). The resulting $g(T)$ is shown in Fig. 8 for q=2 to 6. In this case, $g(T)$ for q=2 and 3 do not intersect, consistent with our previous finding that T_c for these approximants are substantially different. For the larger approximants the lines intersect at a temperature 2.40 in nice agreement with the limiting value of T_c for the approximants. However, since the approximants in the sequence are really *different* periodic lattices, we would like to emphasize again that it is not *a priori* clear how fast the region of the validity of the finite-size scaling should be reached in this case.

To detect a change in the universality class we must study the exponents and the amplitudes as a function of the approximants. Using $L = \sqrt{N}$ as a measure of the linear size of the system and $d = 2$, we estimate $1/\nu$ for the approximants q=2 to 6. In Fig. 9, a log-log plot of $g'(T_c)$ versus L is shown for the q=5 approximant. The T_c used is the one determined above. Using a least squares fit we obtain $1/\nu = 0.99 \pm 0.02$ and $\ln|\tilde{g}'(0)| = -3.073 \pm 0.074$. In Table II, $1/\nu$ are tabulated for the rest of the approximants. No variation with q is observed for ν, and the estimated values agree very well with the exact value for the two-dimensional Ising model, $\nu = 1$. This is consistent with the assumption that all rational approximants are periodic and, thus, belong to the same universality class, i.e., that of the Ising model on periodic

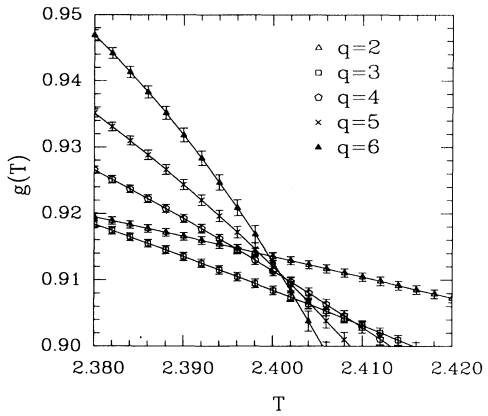

FIG. 8. $g(T)$, defined in the text, as a function of T for different rational approximants with q =2 to 6. All the lines are for systems of 2×2 unit cells. In all cases 5×10^6 MC/S were performed. The simulation temperature was 2.40.

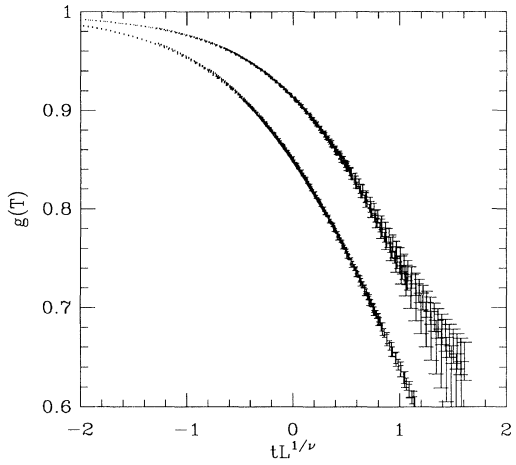

FIG. 10. Scaling plot of $g(x)$ as a function of $tL^{1/\nu}$. The top curve is for periodic boundary conditions, i.e., the rational approximants. Only the results for q=5 are shown. The lower curve is for toroidal boundary conditions. The results for spherical boundary conditions are not shown since they fall essentially on top of the results for toroidal boundary conditions.

lattices. In particular $\tilde{g}$, and therefore $\tilde{g}'(0)$, should be the same for all the approximants. In Fig. 10 a plot of $g(x)$ as a function of $tL^{1/\nu}$ is shown for the $q = 5$ approximant. The values used for T_c and ν are the ones obtained above. For other values of q the same plot falls essentially on top of this one and are not shown for clarity. For the smaller approximants q=2,3 the curve appears marginally shifted upward.

A log-log plot of $\langle M^2 \rangle|_{T=T_c(q)}$ versus L is shown for the $q = 5$ approximant in Fig. 11. A linear fit leads to $\eta = 0.250 \pm 0.003$, in complete agreement with the 2D Ising value, $\eta = \frac{1}{4}$. For the remaining approximants studied, the obtained exponents can be found in Table II. Again no significant variation with q is observed for η. We therefore confirm that the approximants belong to the same universality class, i.e., that of the two-dimensional Ising model on periodic lattices.

We must now study the amplitudes associated with the critical behavior, A_0, $\chi_\pm$, etc., in order to detect a possible change in the universality class at $q = \infty$. Using Eq. (18) we determined A_0 for each q as the slope of the straight line in a semilog plot of the specific heat at $T_c(q)$ as a function of the linear size of the system. The results are shown in Fig. 12, with the corresponding values listed in Table II. For $q = 1$, A_0 must take the Ising value. As previously discussed, a determination of A_0 by use of Eq. (18) also gives the critical amplitude, defined in Eq. (19), since the two, in this case, are the same. Therefore A_0 should be independent of the boundary conditions used. Assuming that $A_0(q)$ will tend toward a finite value as $q \to \infty$, we plot $A_0(q)$ against $1/q$. It is seen that the specific heat amplitude, while decreasing, indeed converges to a finite value as $q \to \infty$. Thus, we must conclude that the Penrose lattice displays the same logarithmic divergence of the specific heat as does the square lattice Ising model. Hence, the exponent α is equal to 0 in both cases, although the associated amplitude is different.

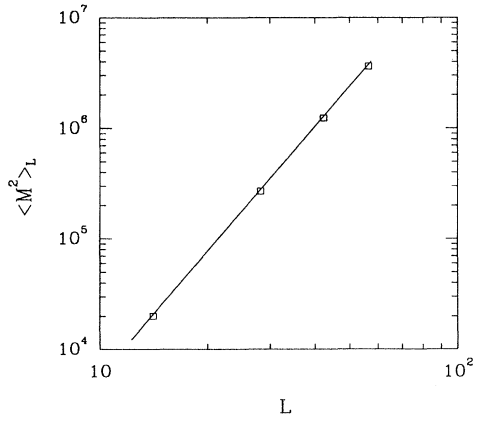

FIG. 11. $\langle M^2 \rangle$ as a function of $L = \sqrt{N}$ for the $q = 5$ approximant. The points shown are for linear sizes of 1, 2, 3, and 4 unit cells, with N equal to 199, 796, 1791, and 3184, respectively. In all cases 3×10^6 MC/S were performed. The error bars are smaller than the points shown. The simulation temperature was 2.39.

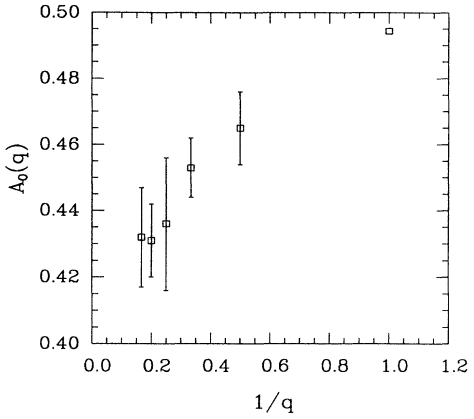

FIG. 12. The specific heat amplitude A_0 at $T_c(q)$ as a function of $1/q$. The $T_c(q)$ used is as determined from the analysis of $g(T)$ for each q.

Using the values for $T_c(q)$ previously obtained, we extract χ_0 from log-log plots of the susceptibility as a function of the linear system size, where $\chi_0 = M_0^2/T_c$ with χ_0 and M_0^2 defined in Eqs. (17) and (24). We have already established that the exponent η is the same for the different approximants, thus we expect parallel straight lines with the slope $2 - \eta$ to be present in a log-log plot. A variation in the amplitude χ_0, with q, would separate the lines for different approximants. As mentioned above, χ_0 is proportional to $\chi_\pm$ through a constant depending on the boundary conditions used. Thus a change in $\chi_\pm$ will be reflected in χ_0. The interest is thus in the intercept, $\ln \chi_0$, whose divergence in the limit $q \to \infty$ would reveal a crossover to a different universality class. The results can be found in Table II. No significant variation with q is observable. From this we verify that η retains the usual Ising value also in the limit of the Penrose lattices. Due to the scaling relations, the two exponents, α and η, are enough to determine the universality class and we must conclude that the Ising model on Penrose lattices belongs to the same universality class as the two-dimensional Ising model on periodic lattices.

The above analysis of the rational approximants demonstrates that the Ising model on Penrose lattices is in the same universality class with the Ising model on periodic lattices. In order to verify this conclusion, and to investigate effects of different boundary conditions, we have performed similar simulations for toroidal and spherical boundary conditions.

B. Toroidal and spherical boundary conditions

The results for $g(T)$ are shown in Fig. 13. Although the intersection determining T_c is not as well defined as for the rational approximants, the obtained values of $T_c = 2.398 \pm 0.002$ for toroidal and $T_c = 2.398 \pm 0.004$ for spherical boundary conditions are clearly consistent with the results $T_c = 2.401 \pm 0.005$ for the $(\infty \times \infty)_\infty$- and $T_c = 2.400 \pm 0.002$ for the $(2\times2)_\infty$-periodic boundary con-

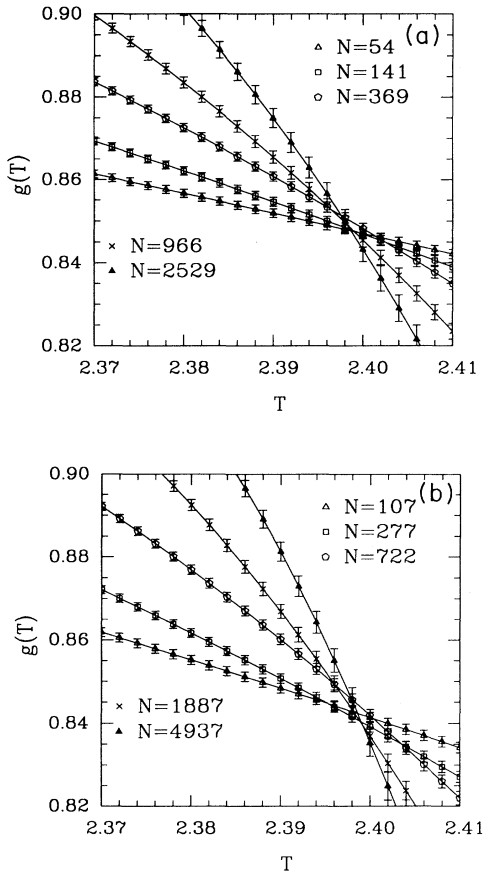

FIG. 13. (a) $g(T)$, defined in the text, as a function of T for toroidal boundary conditions. The lines shown are for systems consisting of 54, 141, 369, 966, and 2529 spins, respectively. In all cases 5×10^6 MC/S were performed. The simulation temperature was 2.40. (b) $g(T)$, as a function of T for spherical boundary conditions. The lines shown are for systems consisting of 107, 277, 722, 1887, and 4937 spins, respectively. In all cases 5×10^6 MC/S were performed. The simulation temperature was 2.40.

ditions. For toroidal and spherical boundary conditions we obtain $g^* \simeq 0.845$ and 0.842, respectively. A scaling plot of g as a function of $tL^{1/\nu}$ is shown in Fig. 10 for the toroidal boundary conditions. For the spherical boundary conditions the curve falls almost on top of the one for the toroidal boundary conditions. Since the results for the toroidal boundary conditions collapse better onto a single curve than the results for the spherical boundary conditions, only these are shown for clarity. Surprisingly one finds that the scaling curves for periodic and "aperiodic" boundary conditions are widely separated, a fact also apparent from the values of g^* ($\simeq 0.916$ and $\simeq 0.843$ for periodic and "aperiodic" boundary conditions, respectively).

A determination of the exponents, using the finite-size scaling analysis, results in $\eta \approx \frac{1}{4}$ and $\nu \approx 1$ for both toroidal and spherical boundary conditions (see Table I). Again no change away from the Ising values obtained for the $(\infty \times \infty)_\infty$- and $(2 \times 2)_\infty$-periodic boundary conditions is observed. For the specific heat critical amplitude we obtain a value of $A_0 \approx 0.44$ for both spherical and toroidal boundary conditions. This is in nice agreement with the values $A_0(q) \approx 0.43$ and 0.415 which we found for the $(\infty \times \infty)_\infty$- and $(2 \times 2)_\infty$-periodic boundary conditions, respectively.

For the three different boundary conditions considered one should obtain the same results for T_c, ν, η, and A_0 when one extrapolates to the limit of the Penrose lattices. However, the quantities g^* and χ_0 will depend on the boundary conditions. This is in nice agreement with our results.

As opposed to the rational approximants, the spherical and toroidal boundary conditions in a sense take the quasiperiodicity of the Penrose lattices into account through the boundary conditions. Thus, any change in the critical behavior would be more directly manifested. No change in critical exponents is observed and, thus, we again conclude that the Ising model on Penrose lattices is in the same universality class as the Ising model on periodic lattices.

V. CONCLUSION

New high precision Monte Carlo simulations of the ferromagnetic, zero-field Ising model on Penrose lattices have been performed. By analyzing the data for rational approximants as a function of the approximant, q, we obtain the limiting value of the transition temperature $T_c(q = \infty) = 2.401 \pm 0.005$. The exponents $\eta \approx \frac{1}{4}$ and $\nu \approx 1$ show no significant variation with q. This is to be expected since the approximants are really *periodic* lattices. We emphasize that the proper place to look for a cross-over to a new universality class would be in the limit of infinite q. A change in the universality class would be indicated if one or more of the critical amplitudes either converged to zero or alternatively diverged as $q \to \infty$. While a small decrement in the specific heat critical amplitude is observed as $q \to \infty$, the amplitude saturates at a finite value. Similarly, all other relevant amplitudes converge to finite, nonzero values. From this we can rule out the possibility of a change in the universality class as $q \to \infty$. Consistent results are obtained using spherical, toroidal, and $(2\times2)_\infty$-periodic boundary conditions. Therefore, we conclude that quasiperiodicity of the Penrose tiling does not affect the Ising universality class.

Significant differences are observed between the periodic and "aperiodic," i.e., the spherical and toroidal, boundary conditions. The scaling function $\tilde{g}$ is considerably different in the two cases. A rapid convergence to the finite-size-scaling regime is seen for the toroidal and periodic boundary conditions. Therefore, it seems more appropriate to use the toroidal boundary conditions for finite-size studies of quasicrystals.

It is of interest to study the influence of phason fluctuations on the ferromagnetic transition. Currently such simulations are in progress and will be presented in a sequel to this paper.

ACKNOWLEDGMENTS

We are indebted to A. Peter Young for many stimulating discussions and we would like to thank Thomas L. Madden for many useful comments. Two of us (M.V.J.) and (M.R.) are grateful to the Physics Department, University of California, Santa Cruz, for hospitality during a part of this project. This work was supported in part by NSF Grants No. DMR8821802 and DMR 87-21673, and also partially by the Italian CNR "Progetto Finalizzato Sistemi e Calcolo Parallelo" - U.O. Reatto.

---

*Permanent address: Physics Department, University of California, Santa Cruz, CA 95064.

[1] C. Berger and J. J. Prejean, Phys. Rev. Lett. **64**, 1769 (1990); F. L. A. Machado *et al.*, Solid State Commun. **75**, 1 (1990); D. P. Yang *et al.* (unpublished).
[2] Y. Achiam, T. C. Lubensky, and E. W. Marshall, Phys. Rev. B **33**, 6460 (1986).
[3] H. Tsunetsugu and K. Ueda, Phys. Rev. B **36**, 5493 (1987).
[4] J. M. Luck, J. Phys. C **3**, 205 (1986).
[5] Th. M. Nieuwenhuizen, J. Phys. C **3**, 211 (1986).
[6] C. Godréche, J. M. Luck, and H. Orland, J. Stat. Phys. **45**, 777 (1986).
[7] I. Bose, Phys. Lett. A **123**, 224 (1987).
[8] A. Doroba and K. Sokalski, Phys. Status Solidi B **152**, 275 (1989).
[9] R. Abe and T. Dotera, J. Phys. Soc. Jpn. **58**, 3219 (1989).
[10] A. Doroba (unpublished).
[11] C. A. Tracy, J. Phys. A **21**, L603 (1988).
[12] G. Amarendra, G. Ananthakrishna, and G. Athithan, Europhys. Lett. **5**, 181 (1988).
[13] Y. Okabe and K. Niizeki, J. Phys. C **8**, 1387 (1988).
[14] V. E. Korepin, Commun. Math. Phys. **110**, 157 (1987).
[15] Y. Okabe and K. Niizeki, J. Phys. A **23**, L733 (1990).
[16] S. M. Bhattacharjee, J.-S. Ho, and J. A. Y. Johnson, J. Phys. A **20**, 4439 (1987).
[17] Y. Okabe and K. Niizeki, J. Phys. Soc. Jpn. **57**, 16 (1988).
[18] Y. Okabe and K. Niizeki, J. Phys. Soc. Jpn. **57**, 1536 (1988).
[19] N. G. deBruijn, Ned. Akad. Weten. Proc. Ser. A **43**, 39 (1981); **43**, 53 (1981); M. V. Jarić, Phys. Rev. B **34**, 4685 (1986).
[20] L.-H. Tang and M. V. Jarić, Phys. Rev. B **41**, 4524 (1990).
[21] There are many ways of constructing similar sequences. The simplest one is to use inflations of the elementary hexagons. They consist either of two 72° rhombi and one 36° rhombus, of two 36° rhombi and one 72° rhombus.
[22] A. M. Ferrenberg and R. H. Swendsen, Phys. Rev. Lett. **61**, 2635 (1988).
[23] K. Binder, Z. Phys. B **43**, 119 (1981).
[24] V. Privman, in *Finite Size Scaling and Numerical Simulation of Statistical Systems*, edited by V. Privman (World Scientific, Singapore, 1990), p. 1.
[25] A. E. Ferdinand and M. E. Fisher, Phys. Rev. **185**, 832 (1969).
[26] M. E. Fisher, in *Finite Size Scaling and Numerical Simulation of Statistical Systems* (Ref. 24), p. 173.
[27] M. N. Barber, in *Phase Transitions and Critical Phenomena*, edited by C. Domb and J. Lebowitz (Academic, New York, 1983), Vol. 8, p. 145.